Received June 5, 2020, accepted June 18, 2020, date of publication July 7, 2020, date of current version August 3, 2020.

Digital Object Identifier 10.1109/ACCESS.2020.3007773

Improvement of Low-Speed Precision Control of a Butterfly-Shaped Linear Ultrasonic Motor

YUNLAI SHI[1], (Member, IEEE), JUN ZHANG[1,2], YUYANG LIN[1], (Graduate Student Member, IEEE), AND WENBO WU[1]

[1]State Key Laboratory of Mechanics and Control of Mechanical Structures, Nanjing University of Aeronautics and Astronautics, Nanjing 210016, China
[2]College of Mechanical and Electronic Engineering, Northwest A&F University, Yangling 712100, China

Corresponding author: Jun Zhang (junzhang@nwafu.edu.cn)

This work was supported by the National Natural Science Foundation of China under Grant 51975282.

ABSTRACT The control performance of a butterfly-shaped linear ultrasonic motor is not good when the target speed is less than 1 mm/s by traditional methods. To improve low-speed controlling characteristics of linear ultrasonic motor, a closed-loop control strategy by using both the step control and the fuzzy PID control was proposed. The controller was constructed with the function of providing a closed-loop control of the speed by adjusting the driving voltage amplitude in stepping driving mode. The corresponding step controlling parameters were determined by experiments. Comprehensive experiments on the developed control strategy were conducted under different target speeds. There was a maximum of 24.5% speed error at the target speed of 10 μm/s, meanwhile, the coefficient of variation and the response time were 16.3% and 0.11 s, respectively. With the triangular or sinusoidal waves speed tracking curves at amplitude of 1 mm/s, the maximum speed tracking error were 0.1 mm/s and 0.15 mm/s respectively. Thus, a good speed tracking performance was obtained. These results support the functional ability and potential of the proposed method as a low-speed precision control method for linear ultrasonic motors.

INDEX TERMS Linear ultrasonic motor, step control, fuzzy PID control, low speed.

NOMENCLATURE

C_v	Coefficient of variation
e_m	Maximum speed error of the platform
$e(t)$	Speed error of the platform
$\dot{e}(t)$	Change of speed error of the platform
K_p	Proportional coefficient of the PID controller
K_p^0	Initial value of proportional coefficient
ΔK_p	Change of proportional coefficient
K_I	Integral coefficient of the PID controller
K_I^0	Initial value of integral coefficient
ΔK_I	Change of integral coefficient
K_D	Differential coefficient of the PID controller
K_D^0	Initial value of differential coefficient
ΔK_D	Change of differential coefficient
N_d	Number of driving waves of the driving signal
$r(t)$	Set speed of the platform
R^2	Coefficient of determination
T_d	Driving period of the driving signal
$\bar{v}$	Average speed of the platform
$y(t)$	Actual position of the platform
$\dot{y}(t)$	Actual speed of the platform
σ	Standard deviation of the platform speed

The associate editor coordinating the review of this manuscript and approving it for publication was Kan Liu.

I. INTRODUCTION

A linear ultrasonic motor (LUSM) is a special type of motor by using the inverse piezoelectric effect and ultrasonic vibration. The motor converts the micro-deformation of elastic material into the motion of the slider through friction coupling [1]. During the past decades, a significant interest has arisen in the issue of using LUSM for precise positioning [2]–[4]. The motivation of these efforts is the attractive features of the LUSMs, such as quick response, electromagnetic immunity, and off power self-locking. Considering these excellent characteristics, LUSMs have broad application prospects in fields of optical precision platform, micro-nano operation system and precision measurement system [4]–[8].

However, in many applications such as semiconductor device inspection, the requirements for both long stroke, rapid and high positioning accuracy should be satisfied. This means

that the motor must have a certain speed to ensure that the platform can be quickly driven to the target position, however, to achieve high positioning accuracy, the speed cannot be fast, the two goals are in conflict. Therefore, the speed of the motor should be decreased to a stable low value before reaching the target position to achieve high-precision positioning. Indeed, a low speed is necessary for microscopy stages, robotic arms, medical operations, and so on. To enable high precision control of the LUSM, various control strategies have been investigated [9]–[14], such as model predictive control, fuzzy neural networks, nonlinear PID and sliding mode.

In most cases, many LUSMs are resonating displacement devices for which the alternating strain of its stator is excited by an AC field at the mechanical resonance frequency, which can provide long stroke (no limited in theory) and can easily reach the speed of greater than 100 mm/s. However, these types of motors are difficult to achieve low speed precision control due to the obvious nonlinearity of the motor and the velocity dead zone of the motor. The motion of the motor can only be achieved when the driving voltage above a threshold voltage level, which causes much trouble with the low speed control of the LUSM.

Chu *et al.* proposed a differential composite motion method to achieve the speed or the step size controlling of a rotary ultrasonic motor by adjusting the duty ratio of driving signal and the displacement difference between the clockwise and counterclockwise rotation [15]. A minimum stepped angle of was obtained by using this method. Zhang *et al.* developed a PWM control method to realize the low speed controlling of a linear ultrasonic motor by adjusting the difference of the two vibrators' vibrating amplitudes [16]. This method is different from the general method of decreasing vibrating amplitude of ultrasonic motor to realize low speed, two transducers of the linear ultrasonic motor are respectively excited by pulses whose width can be modulated to realize two contrary elliptical vibrations with different vibrating amplitudes. The minimum speed of 0.1 mm/s was realized by driving an aerostatic guide. Zeng *et al.* proposed a superposition pulse driving approach of rotary ultrasonic motor for control moment gyro servo system [17]. The superposition pulse driving method, which prolong the turn-off time of the traditional step driving method, includes the traveling wave area and the standing wave area. However, the velocity fluctuation reaches 47.3% at the motor speed of 0.28°/s by this method.

In this study, to realize a smooth lower speed control of a butterfly-shaped LUSM, a closed-loop control strategy by using both the step control and the fuzzy PID control was proposed. This paper is organized as follows: a motion table driven by the butterfly-shaped LUSMs and its corresponding control system is presented in section II for using it to study the speed control characteristics of LUSM. Then, the corresponding control strategy for low speed control of LUSM is proposed in section III, followed in section IV by the experiments associated with the Low speed control and tracking characteristics. Finally, the conclusion of this study is presented in section V.

II. DESCRIPTION OF THE PLATFORM SYSTEM

In this study, a butterfly-shaped LUSM developed by authors is utilized for studying the low speed control characteristics [2], [18]. Two specially selected vibration modes of the motor stator, symmetric and anti-symmetric modes, are activated at the same time to realize elliptical motion on the driving foot of the motor stator by using the d_{33} effect of the piezoelectric ceramic. In most case, the stator of the LUSM can be matched with different structures as movers according to the application requirements. Here, to verify the effectiveness of the proposed control strategy, a two DOF motion platform driven by the butterfly-shaped LUSMs is taken as a research object (see Fig. 1). It consists of the upper stage, the lower stage, the middle stage. Here, the upper stage and the lower stage are regarded as LUSM's movers. Two butterfly-shaped piezoelectric stators are mounted on the middle stage to match the upper and lower stages. Four commercially available crossed roller rails are applied as the guide rail, and two ceramic strips, adhered on the upper and lower stages, play the role of contacting with the driving feet of the stator and transfer the motion to the upper and lower stages. Here, a linear encoder (JENA LIA20, NUMERIK Ltd., Germany) with the resolution of 10 nm is used as the displacement feedback element. The dimension of the stage is 162 mm×162 mm×52 mm.

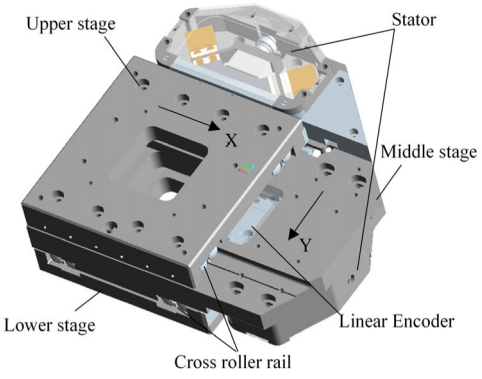

FIGURE 1. The mechanical structure of the motion platform.

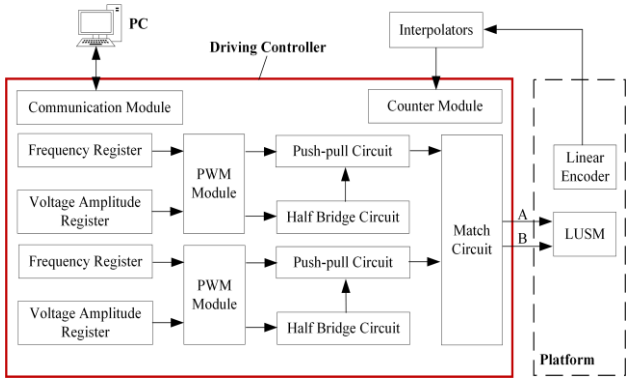

FIGURE 2. Block diagram of the motion platform system.

The block diagram of the driving and controlling system of the motion platform is shown in Fig. 2. A driving controller developed by authors is used to generate the driving signals of the motor and implement the control strategies [19]. By using this device, the driving voltage and the driving frequency of the motor can be adjusted in time. A PC is used to communicate with the driving controller by a serial port interface. The interpolator (IPE2000-USB, GEMAC Ltd., Germany) is used to increase the resolution for incremental position and angular measuring systems with sinusoidal output signals offset by 90°. The driving controller can get the displacement of the platform by the RS422 output signals. According to the command of the PC and the feedback of linear encoder, the frequency register and the voltage amplitude register are adjusted by proposed algorithm so as to control the speed of the LUSM. The characteristics of the motion platform system is shown in Table 1. The corresponding characteristic parameters were tested by the National Institute of Metrology of China.

TABLE 1. Characteristics of the motion platform system.

Parameter	Value	Parameter	Value
Travel	50 mm	Repositioning Accuracy	±0.3 μm
Traversing rate	⩽200 mm/s	Max. acceleration	5 g
Position accuracy	±0.5 μm	Permissible load	F_x=10 N; F_y=15 N; F_z=30 N;

III. CONTROL STRATEGY FOR LOW SPEEDS

Here, the speed of the LUSM can be controlled by the driving voltage, frequency and the phase difference of the two-phase power sources. Ideally, the frequency response of the operation modes of LUSM (symmetric and antisymmetric mode) should be the same. However, the frequency response of the two operation modes is inconsistent due to machining and assembly errors. Therefore, it is not appropriate to adjust the motor speed by changing the driving frequency. Since changing driving voltage method supports better linearity than other methods, the LUSMs are often controlled by this method.

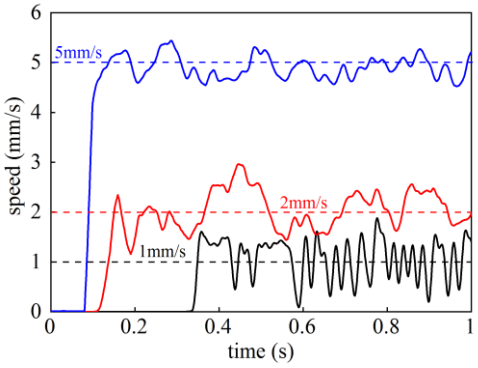

FIGURE 3. The closed loop speed control characteristics of the motor using traditional PID control method at different target speed.

The closed loop controlling features of the motor was tested in low speed zone by using traditional PID control method, the speed of the motor was regulated by adjusting driving voltage applied on the stator of the motor in continuous operation mode. The experimental results at different target speed (1 mm/s, 2 mm/s and 5 mm/s) are shown in Fig. 3. Obviously, the low speed performance goes worse with the target speed decreasing due to an inevitable velocity dead zone caused by the friction between the slider and the stator. The speed fluctuates from 0 to 2 mm/s when the target speed is set to 1 mm/s. Therefore, in order to avoid the dead zone problem and improve the low speed characteristics of the butterfly-shaped LUSM, we consider adopting step control to realize lower speed control.

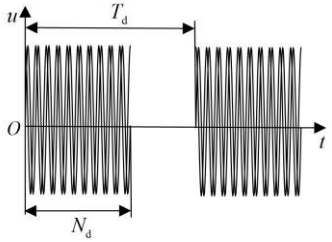

FIGURE 4. Driving signal of step control.

A. STEP CONTROL

To realize step control of the motor, the number of driving waves N_d during driving period T_d is controlled by the driving controller, and a discontinuous driving signal can be produced, as shown in Fig. 4. Thus, the motion of the motor is discontinuous, and a low average speed could be achieved. In this case, however, the speed vary greatly. Therefore, a further study on step characteristics of the motor is performed.

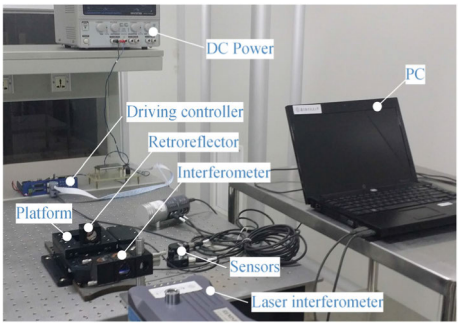

FIGURE 5. Measurement system of the platform.

Figure 5 shows the measurement system for step characteristics of the motor under open loop condition. A laser interferometer (XL-80 Laser Measurement System, Renishaw Ltd., England) with linear measurement accuracy of ±0.5 ppm is used to test the displacement of the platform. The experiments are carried out in the clean room with grade of 10^5 and vibration isolation has been effectively done. During the experiments, the motion of the upper platform is measured, and the driving frequency of the motor is 53.38 kHz.

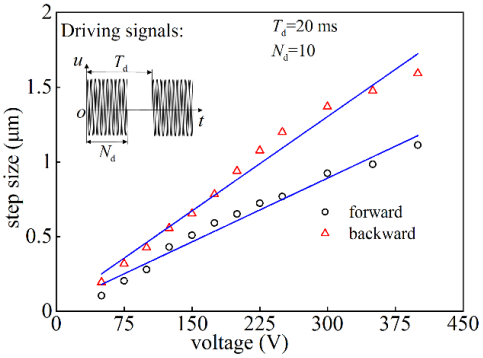

FIGURE 6. Influence of the driving voltage on step size.

Figure 6 shows the influence of the driving voltage on step size. Here, the number of driving waves is 10, and the driving period is 20 ms. Experimental results show that a good linearity between the step size and the driving voltage is obtained, and the coefficient of determination is greater than 0.98. Obviously, there are different paces at the forward and backward direction, due to the assembly error of the motor in both directions. When the driving voltage is 50 V, the average step size at forward and backward direction are 0.105 μm and 0.196 μm.

Moreover, the displacement characteristics of the motor by different driving period were investigated in open loop state (see Fig. 7).

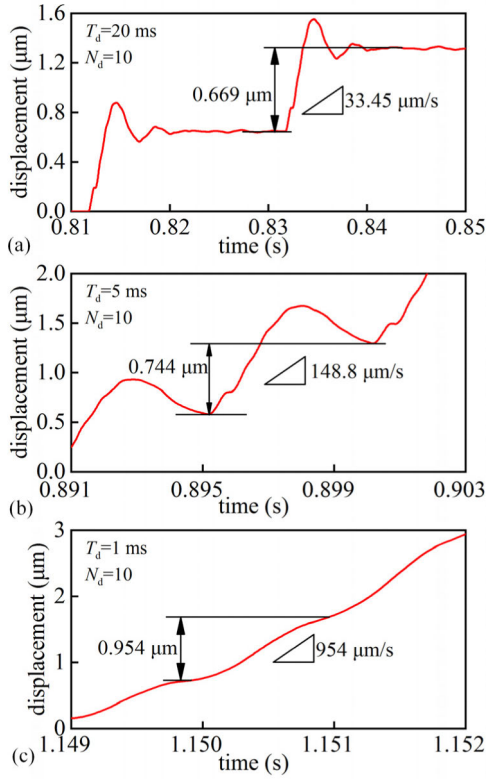

FIGURE 7. Step displacement characteristics of the motor with different driving period. (a) 20 ms. (b) 5 ms. (c) 1 ms.

Here, the driving voltage was set to 200 V, and the number of driving wave was also set to 10. The experiment results show that the step displacement increases from 0.669 μm to 0.954 μm and the average speed increases from 33.45 μm/s to 954 μm/s as the driving period decreasing from 20 ms to 1 ms. Obviously, the longer the driving period, the lower the average speed but the larger the speed fluctuation. When the driving period is 1 ms, the step characteristic becomes inconspicuous and thus the displacement curve becomes smoother.

Accordingly, it can be seen from Fig. 6 and Fig. 7 that it is possible to achieve low speed control with good performance by adjusting the driving voltage in stepping operation mode. Here, considering the smoothness of the speed of the motor in low speed zone, the value of the driving period was set to 1 ms, the number of driving waves was set to 10, and the driving voltage was selected as the control variable.

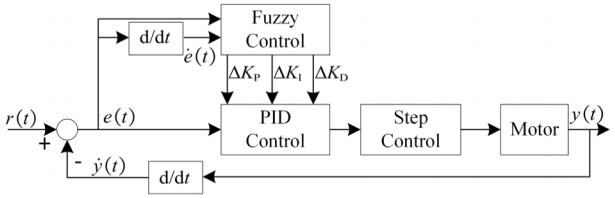

FIGURE 8. Block diagram of the control strategy.

B. FUZZY PID CONTROL

Base on the above experimental results, a fuzzy PID method combined with the stepping operation method were used to regulate the speed of the motor. The block diagram of the control strategy is shown in Fig. 8. The actual position of the platform $y(t)$ is measured by the linear encoder. The speed error $e(t)$ is the difference of the set speed $r(t)$ and the actual speed $\dot{y}(t)$. The fuzzy control updates the parameters of the PID control, and the driving voltage is controlled by the PID control. Then, a discontinuous driving signals with the designed driving period and the desired driving voltage is generated by the step control to power the motor.

The fuzzy controller has two inputs and three outputs. The input signal consists of speed error $e(t)$ and the change of speed error $\dot{e}(t)$. The output signals are composed of ΔK_P, ΔK_I and ΔK_D, which are used to adjust the PID parameters. The PID coefficients of K_p, K_I and K_D could be updated during each control loop based on the following formulas:

$$\begin{cases} K_p = K_p^0 + \Delta K_p \\ K_I = K_I^0 + \Delta K_I \\ K_D = K_D^0 + \Delta K_D \end{cases} \quad (1)$$

where K_p^0, K_I^0 and K_D^0 are the initial values of PID parameters, which could be set by traditional PID method and practical experience. According to the fuzzy rules, the optimal control signals are produced by these inputs to control the output of the motor driver.

As we know, the fuzzy variables should be quantized to implement fuzzy control, and then the fuzzy variables are

transformed from a basic domain into a fuzzy domain. Generally, the larger the quantization grades of the fuzzy variables, the better the control quality of the system. Considering the amount of calculation, memory occupation, response time and overshoot synthetically, the input signals and output signals of the fuzzy controller were quantized into 15 grades: $\{-7, -6, -5, -4, -3, -2, -1, 0, 1, 2, 3, 4, 5, 6, 7\}$. During the process, the basic domain of $e(t)$ was $[-1, 1]$ mm/s, and the basic domain of $\dot{e}(t)$ was $[-50, 50]$ mm/s^2, the basic domain of ΔK_{p} was $[-0.3, 0.3]$, and the basic domain of ΔK_{I} was $[-20, 20]$, and the basic domain of ΔK_{D} was $[-0.002, 0.002]$.

According to the control performance of the motor, the fuzzy subset of inputs and outputs variables based on linguistic are described as follows: NB (Negative Big), NM (Negative Medium), NS (Negative Small), ZO (Zero), PS (Positive Small), PM (Positive Medium), and PB (Positive Big). The inputs and outputs of the fuzzy controller took the same membership functions, as shown in Fig. 9. The Gaussian functions are used in fuzzy subsets NB and PB, and the trigonometric functions are used in the other fuzzy subsets.

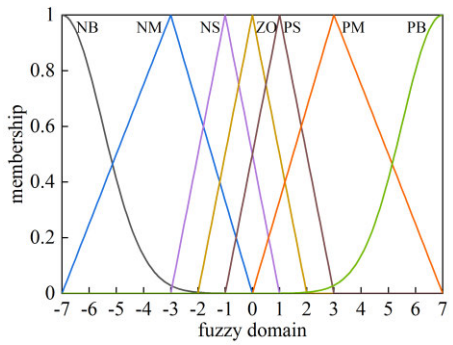

FIGURE 9. Membership function.

According to the tuning principles of PID parameters and engineering experience, a fuzzy PID if-then rule with total of $7 \times 7 = 49$ rule bases for each output was established, as shown in Tables 2-4. Where E and EC are terms in discrete domain of speed error $e(t)$ and the change of speed error $\dot{e}(t)$ after the quantization. Here, the Mamdani fuzzy approach was used.

TABLE 2. Fuzzy rule table for ΔK_{p}.

E	EC						
	NB	NM	NS	ZO	PS	PM	PB
NB	PB	PB	PM	PM	PS	ZO	ZO
NM	PB	PB	PM	PS	PS	ZO	NS
NS	PM	PM	PM	PS	ZO	NS	NS
ZO	PM	PM	PS	ZO	NS	NM	NM
PS	PS	PS	ZO	NS	NS	NM	NM
PM	PS	ZO	NS	NM	NM	NM	NB
PB	ZO	ZO	NM	NM	NM	NB	NB

Based on the analysis above, the output surfaces of each output variable of ΔK_{p}, ΔK_{I} and ΔK_{D} are shown in Fig.10.

TABLE 3. Fuzzy rule table for ΔK_{I}.

E	EC						
	NB	NM	NS	ZO	PS	PM	PB
NB	NB	NB	NM	NM	NS	ZO	ZO
NM	NB	NB	NS	NS	NS	ZO	ZO
NS	NB	NM	NS	NS	ZO	PS	PS
ZO	NM	NM	NS	ZO	PS	PM	PM
PS	NM	NS	ZO	PS	PS	PM	PB
PM	ZO	ZO	PS	PS	PM	PB	PB
PB	ZO	ZO	PS	PM	PM	PB	PB

TABLE 4. Fuzzy rule table for ΔK_{D}.

E	EC						
	NB	NM	NS	ZO	PS	PM	PB
NB	PS	NS	NB	NB	NB	NM	PS
NM	PS	NS	NM	NM	NM	NS	ZO
NS	ZO	NS	NM	NM	NS	NS	ZO
ZO	ZO	NS	NS	NS	ZO	NS	ZO
PS	ZO	ZO	ZO	ZO	ZO	ZO	ZO
PM	PB	PS	PS	PS	PS	PS	PB
PB	PB	PM	PM	PM	PS	PS	PB

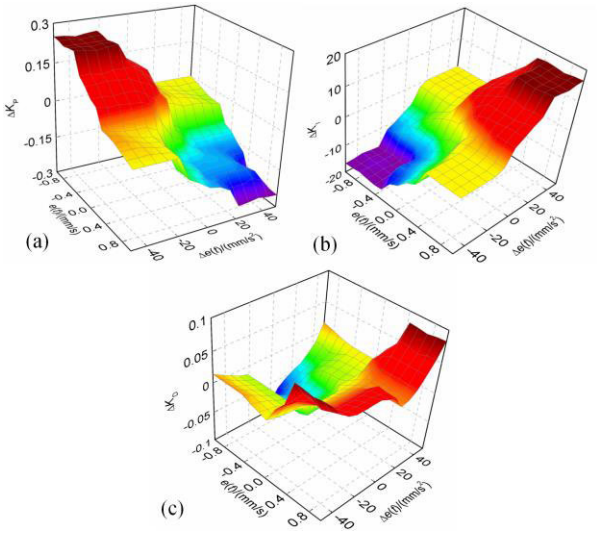

FIGURE 10. Fuzzy surface. (a) ΔK_{p}; (b)ΔK_{I}; (c) ΔK_{D}.

In this study, the center of gravity (COG) method was used to carry out the defuzzification, and the domain of the parameters ΔK_{p}, ΔK_{I} and ΔK_{D} were respectively remapped to the basic domain, then the adjustment values of PID controller were obtained. The driving voltage was adjusted to achieve the speed control according to the calculated PID parameters by (1).

IV. EXPERIMENTAL RESULTS

Comprehensive experiments were carried out by using the proposed control algorithm. Here, the sample frequency was set to 1 kHz. To compare the speed performance at different set speed, the coefficient of variation defined as follow was used:

$$C_v = \sigma / \bar{v} \times 100 \tag{2}$$

where σ is the standard deviation of the speed, and $\bar{v}$ is the average speed of the sample data.

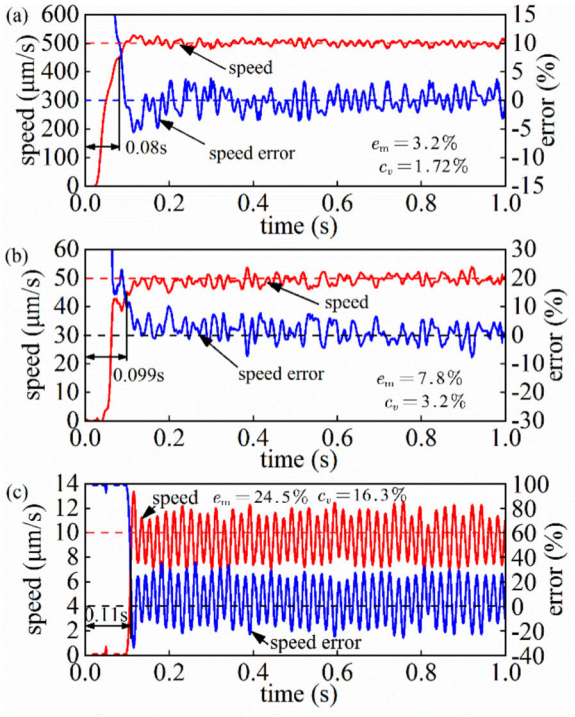

FIGURE 11. Speed characteristics. (a) 500 μm/s. (b) 50 μm/s. (c) 10 μm/s.

From Fig. 11, we can obtained that, as the target speed decreasing, the maximum speed error e_m and the coefficient of variation c_v are respectively increased from 1.72% to 24.5%, and 3.2% to 16.3%, and the response time (defined from zero-speed to 90% target speed) is increased from 0.08 s to 0.11 s. The low speed precision of LUSM is shown in Table 5. Clearly, even at the target speed of 10 μm/s, the maximum speed error e_m and the coefficient of variation c_v in stable state (see Fig. 11(c)) are respectively 24.5% and 16.3%, the relative speed fluctuation amplitude is much smaller than that at the speed of 1 mm/s as shown in Fig. 3 (the motor is controlled by using continuous driving signals).

TABLE 5. Low speed precision of LUSM.

Speed	Speed error e_m	Coefficient of variation c_v	Response time
500 μm/s	3.2%	1.72%	0.08 s
50 μm/s	7.8%	3.2%	0.099 s
10 μm/s	24.5%	16.3%	0.11 s

Figure 12 depicts the low speed tracking characteristics. Here, when the input signal was a triangular wave with period of 1 s and the amplitude of 1 mm/s (see Fig. 12(a)), the maximum speed tracking error was 0.1 mm/s when the ideal speed near zero speed (see Fig. 12(b)).When the input signal was a sinusoidal signal with frequency of 1 Hz and the amplitude of 1 mm/s (see Fig. 12(c)), the speed tracking error performance for the obvious periodical change

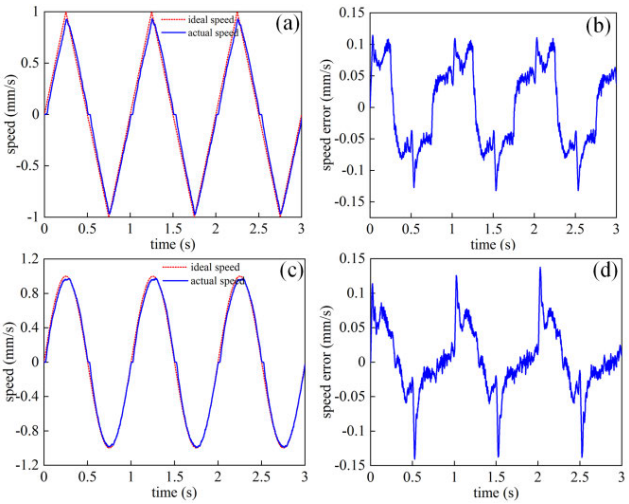

FIGURE 12. FIGURE 12. Low speed tracking characteristics. (a) Triangular wave speed tracking curve. (b) Triangular wave speed tracking error. (c) Sinusoidal wave speed tracking curve. (d) Sinusoidal wave speed tracking error.

characteristics, and the maximum speed tracking error was 0.15 mm/s (see Fig. 12(d)).

V. CONCLUSION

In this paper, we proposed a new control strategy by using both the step control and the fuzzy PID control on low speed control of LUSM in micron scale. Compared to traditional PID controller, the control parameters of fuzzy PID controller were changing by external conditions. Therefore, the fuzzy PID controller is much more suitable for the system with a strong nonlinear and time-variation.

Compared to [16], we developed a different method to achieve a lower speed precision controlling and realized a good results: in this study, the driving voltage of the motor was selected as the control variable and the fuzzy PID control was used to adjust it in real time to achieve low speed control. The minimum speed of the motor achieves 10 μm/s, the maximum speed error and the coefficient of variation c_v in stable state are respectively 24.5% and 16.3%, the maximum speed tracking error of the triangle wave signal and sinusoidal wave signal is respectively 0.1 mm/s and 0.15 mm/s. These results show that the low speed control characteristics of the butterfly-shaped LUSM are beneficial in some applications that need long stroke, fast response and precision positioning. As the butterfly-shaped LUSM is operated in continuous mode, the speed of it can easily achieve over 100 mm/s [18]. Thus, when it is far from the target position, the LUSM can be operated in the continuous operation mode. When approaching the target position, the speed of LUSM can be lowered by using the proposed controlling strategy. Here, the information used by fuzzy PID controller is limited, only the driving voltage of the motor was selected as the control variable. To improve the dynamic performance of the proposed low-speed precision controlling system, the future work is to add the number of driving waves and the driving

period to the control variables. Accordingly, a multi-variable control method should be taken into consideration. Furthermore, we can increase the number of quantization of the fuzzy variables to realize higher accuracy low-speed control if the requirement for system response time is not high.

REFERENCES

[1] C. S. Zhao, *Ultrasonic Motors Technologies and Applications*. Beijing, China: Science Press, 2007, pp. 1–10.

[2] C. Chen, Y. Shi, J. Zhang, and J. Wang, "Novel linear piezoelectric motor for precision position stage," *Chin. J. Mech. Eng.*, vol. 29, no. 2, pp. 378–385, Mar. 2016.

[3] X. Zhou and Y. Zhang, "A new linear ultrasonic motor using hybrid longitudinal vibration mode," *IEEE Access*, vol. 4, pp. 10158–10165, 2016.

[4] Z. Y. Yao, X. Li, R. R. Geng, Y. Jian, Z. Liu, and S. C. Dai, "Advances in design, modeling and applications of linear ultrasonic motors," *J. Vib. Meas. Dig.*, vol. 36, no. 4, pp. 615–622, 2016.

[5] W. Liang, J. Ma, C. Ng, Q. Ren, S. Huang, and K. K. Tan, "Optimal and intelligent motion control scheme for an ultrasonic-motor-driven X-Y stage," *Mechatronics*, vol. 59, pp. 127–139, May 2019.

[6] K. K. Tan, W. Liang, S. Huang, L. P. Pham, S. Chen, C. W. Gan, and H. Y. Lim, "Precision control of piezoelectric ultrasonic motor for myringotomy with tube insertion," *J. Dyn. Syst., Meas., Control*, vol. 137, no. 6, Jun. 2015, Art. no. 64504.

[7] Y.-J. Wang, Y.-C. Chen, and S.-C. Shen, "Design and analysis of a standing-wave trapezoidal ultrasonic linear motor," *J. Intell. Mater. Syst. Struct.*, vol. 26, no. 17, pp. 2295–2303, Nov. 2015.

[8] W. Liang, W. Gao, and K. K. Tan, "Stabilization system on an office-based ear surgical device by force and vision feedback," *Mechatronics*, vol. 42, pp. 1–10, Apr. 2017.

[9] A. Safa, R. Y. Abdolmalaki, S. Shafiee, and B. Sadeghi, "Adaptive non-singular terminal sliding mode controller for micro/nanopositioning systems driven by linear piezoelectric ceramic motors," *ISA Trans.*, vol. 77, pp. 122–132, Jun. 2018.

[10] S. Mu and K. Tanaka, "Position control of ultrasonic motor using PID-IMC combined with neural network based on probability," *Int. J. Appl. Electromagn. Mech.*, vol. 41, no. 1, pp. 59–71, Jan. 2013.

[11] G.-Y. Gu, L.-M. Zhu, C.-Y. Su, H. Ding, and S. Fatikow, "Modeling and control of piezo-actuated nanopositioning stages: A survey," *IEEE Trans. Autom. Sci. Eng.*, vol. 13, no. 1, pp. 313–332, Jan. 2016.

[12] F.-J. Lin, R.-J. Wai, K.-K. Shyu, and T.-M. Liu, "Recurrent fuzzy neural network control for piezoelectric ceramic linear ultrasonic motor drive," *IEEE Trans. Ultrason., Ferroelectr., Freq. Control*, vol. 48, no. 4, pp. 900–913, Jul. 2001.

[13] S. Jingzhuo and W. Huang, "Predictive iterative learning speed control with on-line identification for ultrasonic motor," *IEEE Access*, vol. 8, pp. 78202–78212, 2020.

[14] S. Di and H. Li, "Model-free adaptive speed control on travelling wave ultrasonic motor," *J. Electr. Eng.*, vol. 69, no. 1, pp. 14–23, Jan. 2018.

[15] X. Chu, Z. Xing, L. Li, and Z. Gui, "High resolution miniaturized stepper ultrasonic motor using differential composite motion," *Ultrasonics*, vol. 41, no. 9, pp. 737–741, Mar. 2004.

[16] F. Zhang, W. S. Chen, J. K. Liu, and X. T. Zhao, "Control of an ultrasonic transducer to realize low speed driven," *Ultrasonics*, vol. 44, no. 1, pp. e569–e574, Dec. 2006.

[17] W. Zeng, S. Pan, L. Chen, Z. Xu, Z. Xiao, and J. Zhang, "Research on ultra-low speed driving method of traveling wave ultrasonic motor for CMG," *Ultrasonics*, vol. 103, Apr. 2020, Art. no. 106088.

[18] Y. Shi, Y. Li, C. Zhao, and J. Zhang, "A new type butterfly-shaped transducer linear ultrasonic motor," *J. Intell. Mater. Syst. Struct.*, vol. 22, no. 6, pp. 567–575, Apr. 2011.

[19] J. Zhang, Y. L. Shi, S. Feng, and C. S. Zhao, "Research on micro-step characteristics and excitation signals of linear ultrasonic motor," *Proc. CSEE*, vol. 37, no. 10, pp. 2995–3000, May 2017.

YUNLAI SHI (Member, IEEE) was born in 1976. He received the bachelor's degree in heat treatment from the Shandong University of Technology, China, in 1999, and the Ph.D. degree in mechanical design and theory from the Nanjing University of Aeronautics and Astronautics, China, in 2011. From 1999 to 2004, he was an Engineer with Yankuang Group Ltd. From 2017 to 2018, he worked as a Visiting Professor with the Nano Robotics Laboratory, Polytechnique Montréal. He is currently an Associate Professor with the Nanjing University of Aeronautics and Astronautics. His research interest includes piezoelectric actuation technology and their applications.

JUN ZHANG was born in Anhui, China, in 1987. He received the B.S., M.S., and Ph.D. degrees in mechanical engineering from the Nanjing University of Aeronautics and Astronautics, Nanjing, China, in 2009, 2012, and 2020, respectively. He is currently working with Northwest A&F University, Shaanxi, China. His current research interest includes driving and control techniques of ultrasonic motors.

YUYANG LIN (Graduate Student Member, IEEE) was born in Fujian, China, in 1991. He received the B.S. degree in aircraft manufacture engineering from the Nanjing University of Aeronautics and Astronautics, in 2014, and the M.S. degree in precision instrument and machinery from Huaqiao University, in 2017. He is currently pursuing the Ph.D. degree in mechanical design and theory with the State Key Laboratory of Mechanics and Control of Mechanical Structures, Nanjing University of Aeronautics and Astronautics. His research interests include piezoelectric transducer and ultrasonic motor.

WENBO WU was born in Sichuan, China, in 1996. He received the B.S. degree in aircraft manufacture engineering from the Nanjing University of Aeronautics and Astronautics, in 2018, where he is currently pursuing the M.S. degree in aeronautical engineering with the State Key Laboratory of Mechanics and Control of Mechanical Structures. His research interests include piezoelectric transducers and ultrasonic motors.